

RESEARCH ARTICLE



ISSN: 2321-7758

## EFFECT OF HALFCONE ANGLE ON THE CRUSHING BEHAVIOUR OF GLASS FIBER REINFORCED POLYMER CONICAL FRUSTUM

MULLA MAHAMMAD IRFAN<sup>1</sup>, N.CHARISMA<sup>2</sup>

<sup>1</sup>M.Tech Student in Nimra Institute of Science and Technology, Jupudi, Vijayawada.

<sup>2</sup>Asst.Professor in Mechanical Engineering Department in Nimra Institute of Science and Technology, Jupudi, Vijayawada.



MULLA  
MAHAMMAD IRFAN



N.CHARISMA

### ABSTRACT

The axial compression of thin-walled E-glass fibre/epoxy resin reinforced (GFRP) composite conical frusta was carried out to study the crashworthiness of conical frustum. The hollow frustrated E-glass fibre reinforced polymer (GFRP) conical having semi-apical angle ranging from 15°, 18°, 21° were fabricated using random ply chopped, plain woven roving cross ply [0/90], and oriented mats\*4 layers to the required dimensions as per ASTM standards by hand layup process. The development of surface was created by using CAD tool. By using the surface development a template was prepared. With the template marked on GFRP E-glass fabric. Then rammed with resin hardener mix as per the E-glass gsm. Then chopped the layer on pattern, as per the same 4 layers was mounted on pattern. After curing i.e. 24 hours the GFRP conical frustum was removed from pattern. Now the sharp edge was trimmed as per the ASTM standards. Quasi-static axial compression load was applied over the small end of the conical specimen with a crosshead speed of 2 mm/min using Universal Testing Machine (UTM). From the experiment results, the load deformation characteristics of thin GFRP composite conical shells were analyzed and the results were validated through finite element analysis package ANSYS15.0. Further, the influence of ply orientation and the laminate wall thickness towards the energy absorbing capability of each GFRP conical specimen was studied. The crushing mode of collapse and the failure loads of GFRP composite conical frustums were also investigated to identify the crushing mechanisms involved in thin fibre/resin composite laminated conical specimens under quasistatic axial compression. The different epical halfcone angle of GFRP conical frustums are failed under diff crushing loads. In that 15° halfcone frustum is better compare to other halfcone angles was investigated.

©KY PUBLICATIONS

### I. INTRODUCTION

The fibre laminated composite materials find applications in many fields including the hollow structures of transportation vehicles because of their high specific strength, modulus and high

damping capability. Mostly, the laminated shell structures are introduced in the design of lightweight structures to reduce the total weight of the vehicle without sacrificing its high level of crashworthiness capability. It is necessary to analyze

the crashworthiness of such structural members before implementing it in the actual field. In this regard, the researchers studied the influence of geometry of the structural members, different composite materials and their fibre ply orientation towards the level of crashworthiness. Conducted experimental study on axial crushing of glass fibre composite frustums and found that the frustums with a wall thickness greater than 2 mm, fail by progressive crushing which starts at the small end. Unlike tubular specimens, no trigger is necessary. It is also found that the crashworthiness parameters such as specific energy absorption and absorbed energy of specimen increase with the increase in wall thickness and section diameter but decrease with the increase of the cone semi apical angle in a complex way. Axial collapse of thin-walled fibre glass composite

Conical shells having semi apical angle 15°, 18° and 21°. The results of the study proved that the circular frusta of 15° semi-apical angle show the best crashworthy capability. The results show that the critical buckling load decreases as the semi-cone angle ( $\theta$ ) increases. In critical buckling load is not to a considerable amount. Once semi-cone angle ( $\theta$ ) exceeds as 18° and 21°, the reduction in critical buckling load is to a considerable amount, and it increases up-to 26% for semi apical angle of 18° and also increases up-to 150% for semi apical angle of 21° from initial value of semi-cone angle ( $\theta$ ) 15°. This reduction in buckling strength can be attributed to the change in the geometry of the conical shells. As semi apical angle increases, the radius of the small side of the conical shell gets smaller, and consequently the critical buckling load decreases.

The GFRP conical frustums having 15°, 18° and 21° semi apical angles were tested and the results are exploited in this paper. Further, the performance of GFRP specimens obtained by numerical was taken in FEA in the same failure load point the way of displacement failure as analyzed. With this work to evaluate the level of

crashworthiness capabilities of individual structural members. The corresponding results would be more useful before the implementations of such structural members into the actual field of applications.

## II. FABRICATION OF SPECIMENS

The thin walled GFRP conical test specimens were fabricated by using commercial available 456 gsm mesh density of random, woven roving [0/90°], uni-directional [±60°] ply oriented E-glass fibre mats, and epoxy resin by hand layup method. Initially, three numbers of the conical shaped wooden pattern were prepared as per the specimen category dimensions and they were used as a mould.



Fig. 1 Wooden patterns 15°, 18° and 21°

The outer surface profile of each wooden pattern was traced using a plain cardboard paper as templates to get the required truncated cone profiles. The corresponding individual sections were transferred same as the outer dimensions to woven roving and uni-directional E-glass fibre mats to get the required ply orientated trapezoidal sectional laminas.

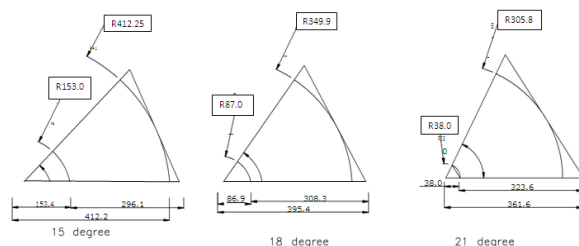


Fig. 2 Surface development of conical frustums

The above dimensions are transferred in plain cardboard paper and the same outer dimensions are marked on fabric.

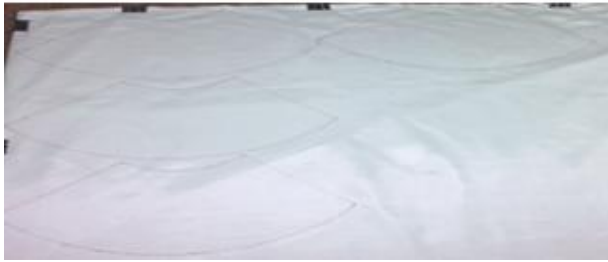


Fig. 3 Transferring the dimension from paper to fabric\*4plys

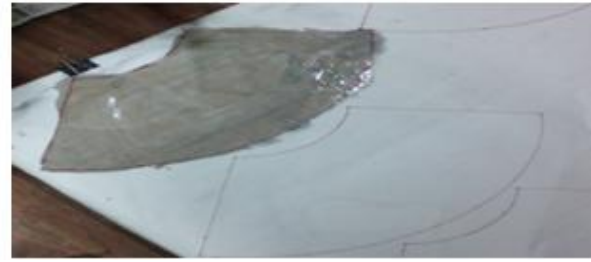


Fig. 4 Applying the matrix on fabric

For the matrix preparation need to calculate the weight of trapezoid fabric for that calculate the aerial density of fabric. With that Ariel density calculate the weight of fabric.

TABLE I: ARIEL DENSITY AND WEIGHT OF FABRIC

No.	Ariel density and weight of fabric		
	Angle of frustum	Ariel density, m <sup>2</sup>	Weight of fabric, g
1	15°	0.1315	63.156
2	18°	0.119	54.264
3	21°	0.1053	48.017

The composition of matrix (resin and hardener) was taken as the proportion with fabric weight is equal to matrix weight; in that resin was taken as 90%weight of fabric and hardener was taken as 10%of resin weight.

TABLE III: COMPOSITION OF FABRIC AND MATRIX

Angle of frustum	Composition of fabric and matrix		
	Fabric weight, g	Resin weight, g	Hardener weight, g
15°	63.156	56.84	6.315
18°	54.264	48.837	5.426
21°	48.017	43.215	4.802

With the above composition of the matrix was taken and stir well continuously for chemical reaction between resin and hardener. As soon as chemical reaction starts heat will appears, in that condition apply immediately the matrix on fabric and apply gently throughout the section uniformly. The matrix will inject in the fabric with the help of smooth edges brush and ram it for injecting the matrix into fabric.

The individual trapezoidal sectional laminas was cut from the fabric and wrapped on the wax coated wooden pattern without air gaps. The matrix

composition was as follows for 1 lamina and the same taken for 4 laminas.

The first ply was placed so that no significant gaps or Overlaps resulted. Similar procedures were adopted to prepare successive plies. During lamination process, extreme care was taken so that the subsequent plies were laid up in-centered with respect to the preceding trapezoidal sectional laminas. At the same time, the outer most of ply was prepared as a single lamina from respective E-glass fibre mat. Then it was over wrapped to encapsulate previous layers or plies. This prevents the building-up of discontinuities through the thickness of the specimen. Similar fabrication process steps were repeated to get the required ply orientated ([0/90°, ±60°]) woven and uni-directional GFRP test specimens.

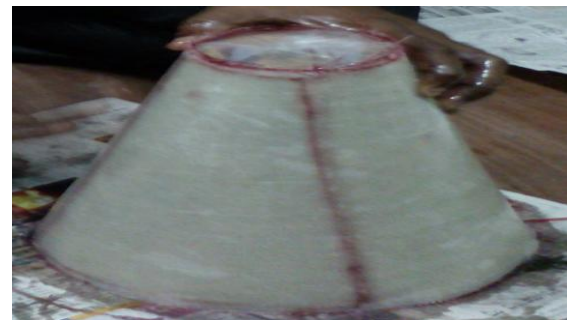


Fig. 5 Fabrication of laminas on wooden pattern

The time should be in control when the arrangement of laminas because when time will delay the matrix will start reaction and the surface will dry. The process will handled at low atmospheric temperature because the atmospheric temperatures will high the chemical reaction is not good between laminas. Keep the total setup at least 24 hours for a better preparation. Remove the moulds from patterns gently. Trim the sharp edges of top and bottom as per the ASTM Standards.

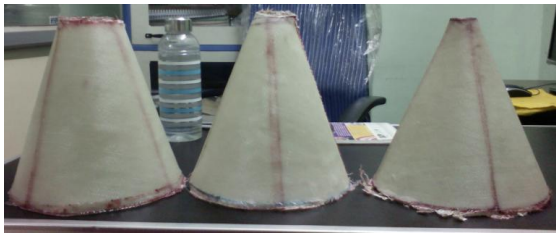


Fig. 6 Specimens after extracting from the moulds  
 Now the specimens after trimming as per the ASTM Standards were prepared for numerical testing.

### III. EXPERIMENTAL PROCEDURE

The specimens were tested both in experimental testing by using UTM and numerical testing by using ANSYS15.0.

#### A. Crushing behaviour under axial compression by UTM

The axial compression test was performed on GFRP conical shell specimen using a computerized Universal Testing Machine (UTM) of 400 KN loading capacity setup. The test specimen was placed in between the top and bottom rigid platens and the proper seating position of specimen was ensured. An axial compression load was applied progressively over the top diameter of GFRP conical specimen with a crosshead speed of 2mm/min. The corresponding load–deformation values were recorded up to failure occurs. The crushing test was conducted with different halfcones of 15°, 18° and 21° then the data was recorded.



Fig. 7 Specimens after experiment by Universal Testing Machine

TABLE IIIII: CRUSHING FAILURE LOAD OBTAINED BY UTM

No.	Crushing failure load obtained by UTM	
	Angle of frustum	Failure load, KN
1	15°	26.640
2	18°	20.492
3	21°	11.312

#### B. Crushing behaviour of axial compression by ANSYS15.0

For the analysis need the properties of E-glass with matrix that resin and hardener. That properties enter the materials that was used for this project on AUTODESK SIMULATION COMPOSITE SOFTWARE and the materials was

- Fabric: E-glass
- Resin:L-12
- Hardener:K-835254

TABLE IV: MATERIAL PROPERTIES

No.	Material properties	
1	Young's Modulus at X- direction,E1	37.722GPa
2	Young's Modulus at Y- direction,E2	9.132GPa
3	Young's Modulus at Y- direction,E3	9.132GPa
4	Poisson's ratio at XY-direction, $\mu_{12}$	0.266
5	Poisson's ratio at XY-direction, $\mu_{23}$	0.427
6	Poisson's ratio at XY-direction, $\mu_{31}$	0.266
7	Modules of Rigidity,G12	3.357GPa
8	Modules of Rigidity,G23	3.199GPa
9	Modules of Rigidity,G31	3.357GPa
10	Compressive Strength,-S1at Fiber direction	-725.00MPa
11	Compressive Strength,-S2	-96.29MPa
12	Density, $\rho$	1937.6

With all this material properties and with the crushing failure load obtained from experimental testing was taken in numerical analysis. At that failure load condition the displacement of failure at each layer was investigated. Fabric has the orientation of two rovings. Each specimen has four laminae.

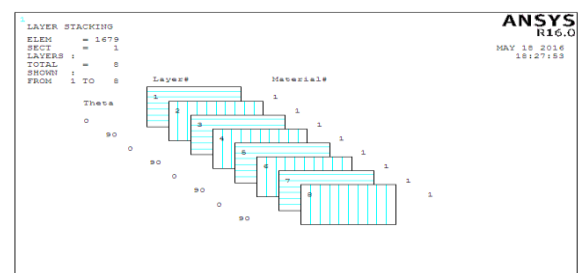


Fig. 8 Orientation of layup

The analysis was carried out by ANSYS15.0  
 1.15° halfcone angle conical frustum crushing analysis

Mesh of the specimen was 8noded 281.

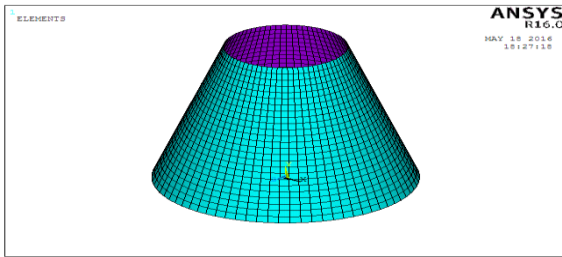


Fig. 9 meshing of specimen

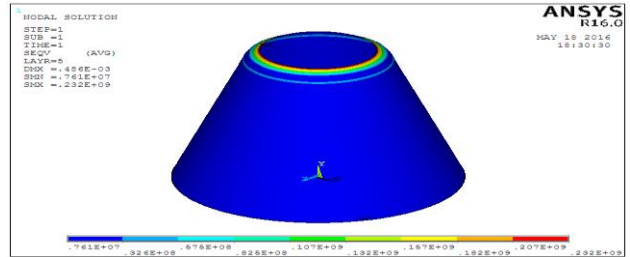


Fig. 14 Displacement on layer 5

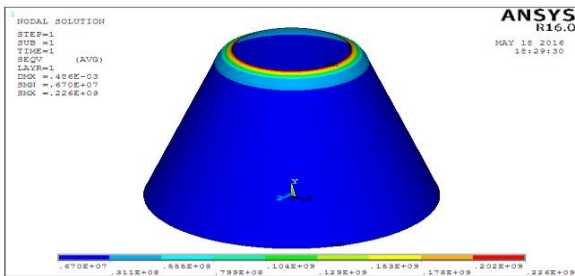


Fig. 10 Displacement on layer 1

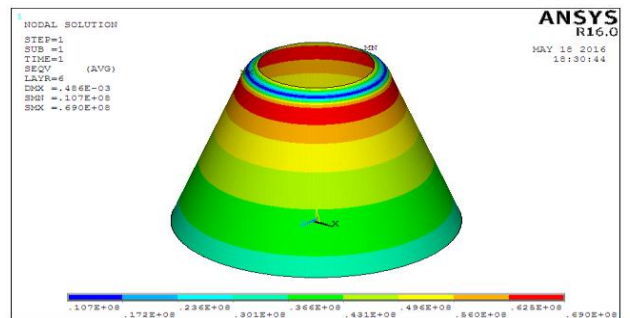


Fig. 15 Displacement on layer 6

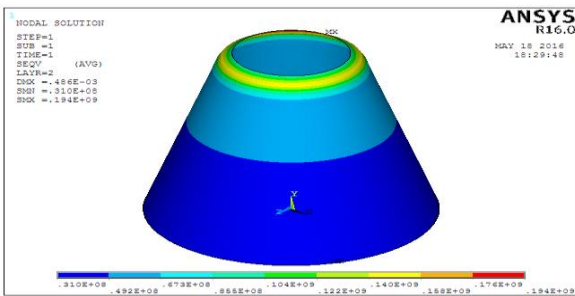


Fig. 11 Displacement on layer 2

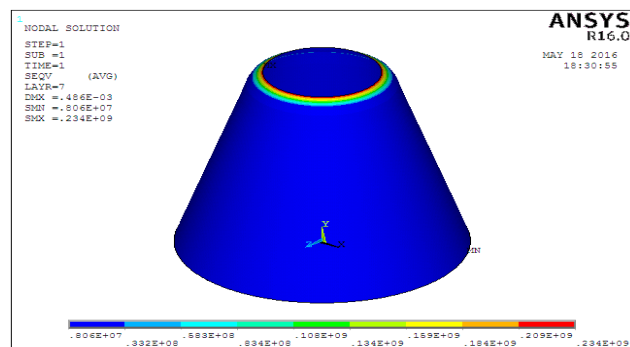


Fig. 17 Displacement on layer 7

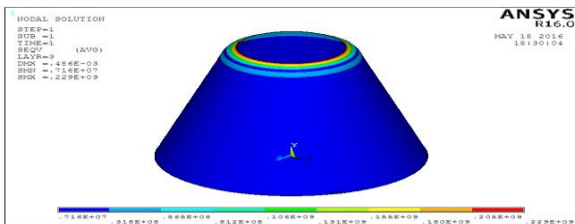


Fig. 12 Displacement on layer 3

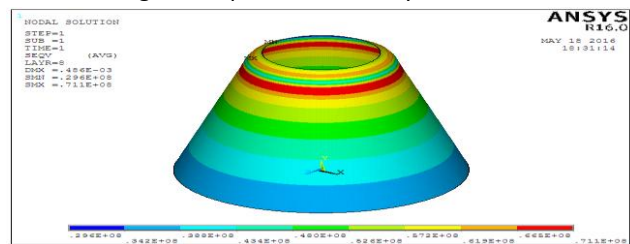


Fig. 18 Displacement on layer 8

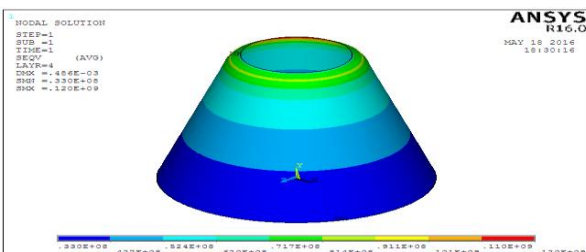


Fig. 13 Displacement on layer 4

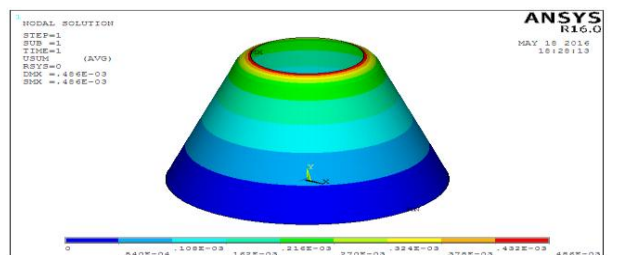


Fig. 19 Total Displacement

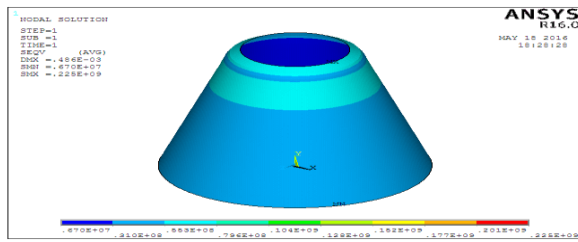


Fig. 20 Equilent stress (Vonmises)  
 2.18° halfcone angle conical frustum crushing  
 analysis

Mesh of the specimen was 8noded 281.

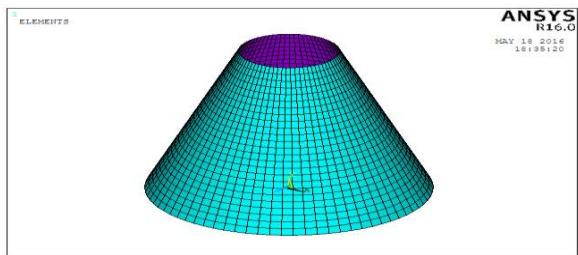


Fig. 21 meshing of specimen

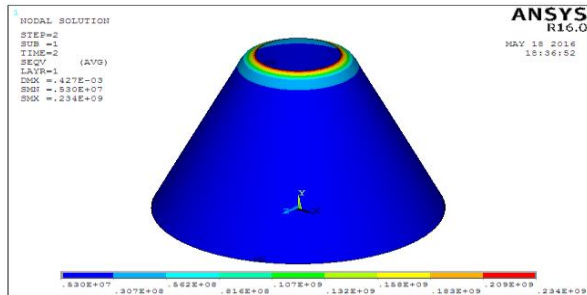


Fig. 22 Displacement on layer 1

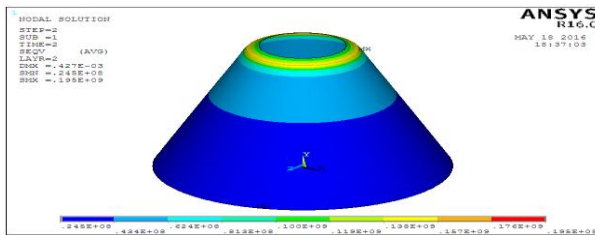


Fig. 23 Displacement on layer 2

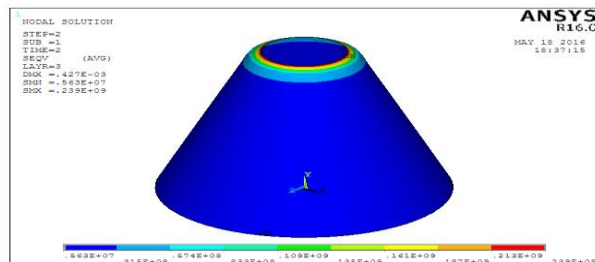


Fig. 24 Displacement on layer 3

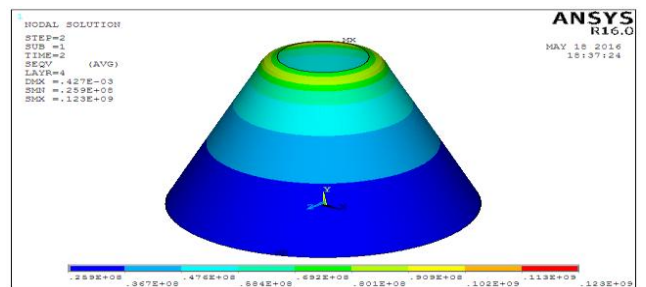


Fig. 25 Displacement on layer 4

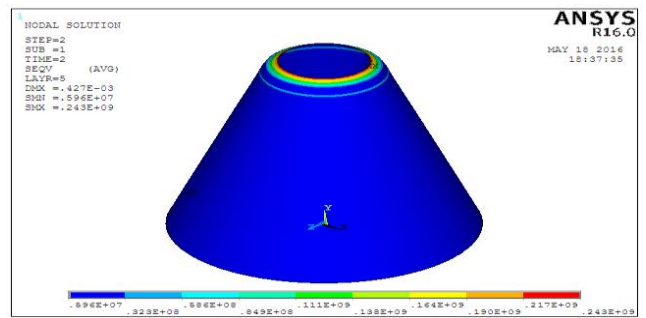


Fig. 26 Displacement on layer 5

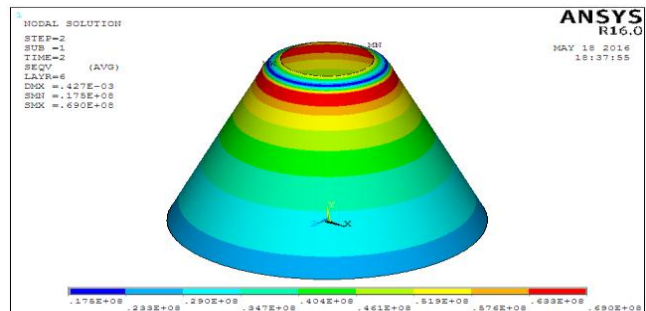


Fig. 27 Displacement on layer 6

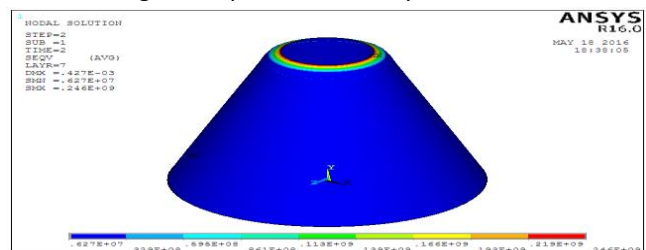


Fig. 28 Displacement on layer 7

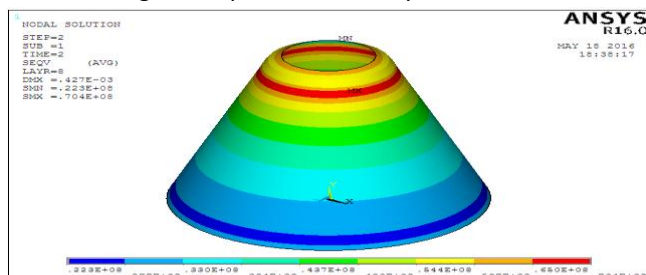


Fig. 29 Displacement on layer 8

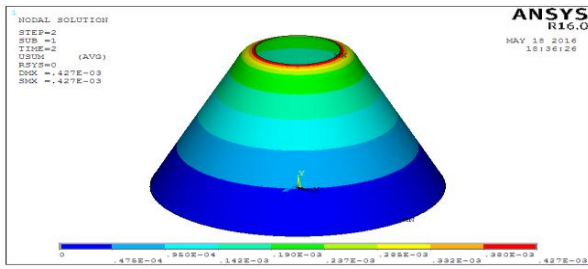


Fig. 30 Total Displacement

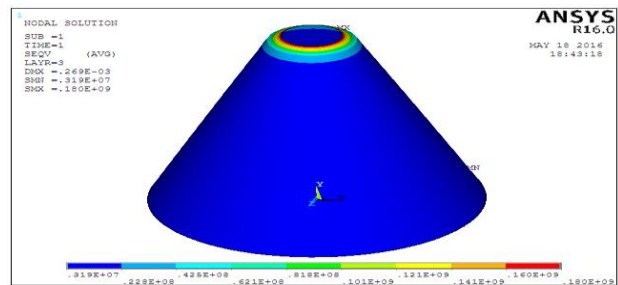


Fig. 35 Displacement on layer 3

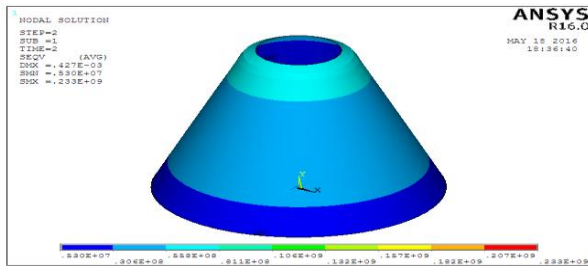


Fig. 31 Equivalent stress (Vonmises)

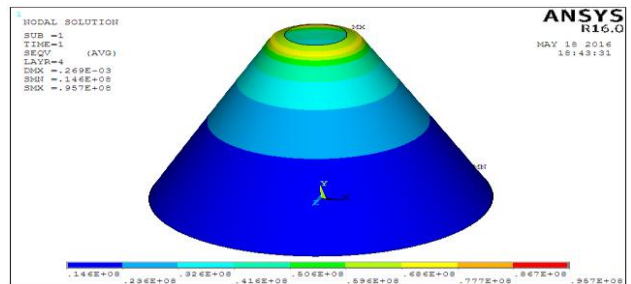


Fig. 36 Displacement on layer 4

3.21° halfcone angle conical frustum crushing analysis

Mesh of the specimen was 8noded 281.

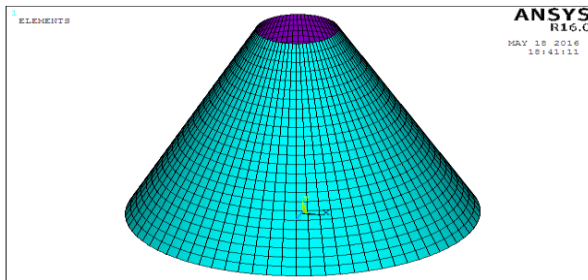


Fig. 32 meshing of specimen

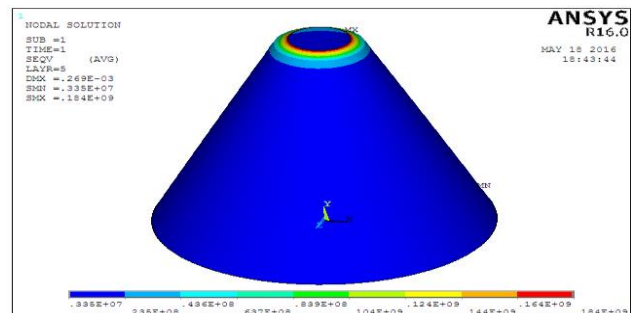


Fig. 37 Displacement on layer 5

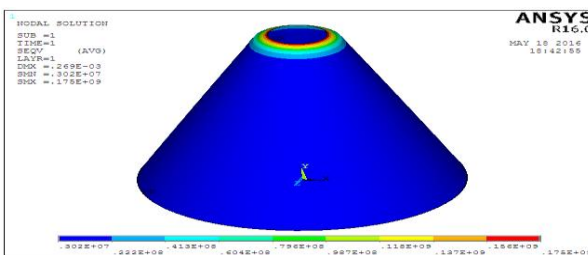


Fig. 33 Displacement on layer 1

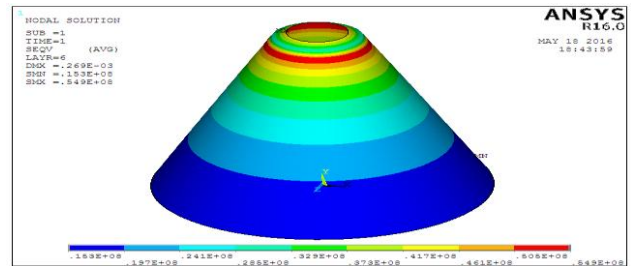


Fig. 38 Displacement on layer 6

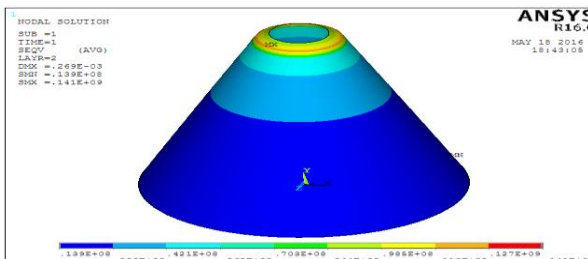


Fig. 34 Displacement on layer 2

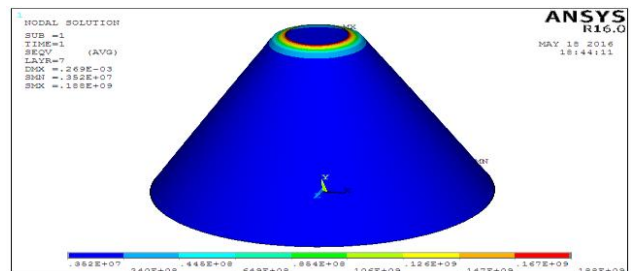


Fig. 39 Displacement on layer 7

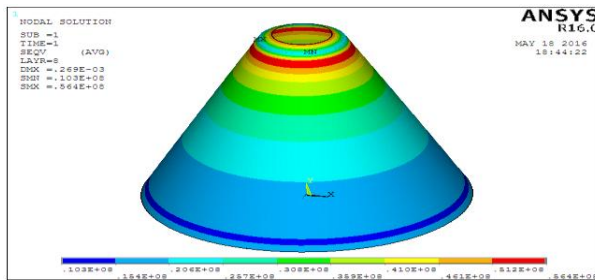


Fig. 40 Displacement on layer 8

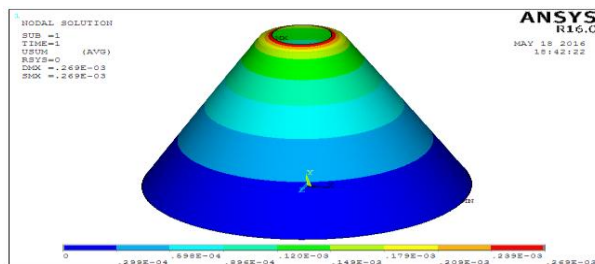


Fig. 41 Total Displacement

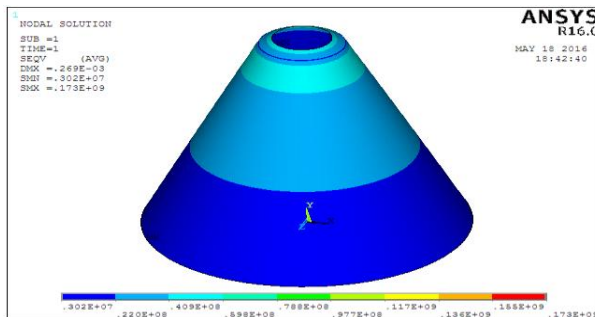


Fig. 42 Equivalent stress (Vonmises)

#### IV. CONCLUSIONS

The energy absorption capability of the specimen is depending on many factors. One of them is the type of material used to fabricate the specimens. Here, three different types of angles were considered to fabricate conical specimens such as 15°, 18°&21°. Composite over wrapped Wooden and the fabricated conical shell specimens were designated with GFRP specimens respectively. The dimensional details of GFRP composite and their experimental test results were retrieved from the corresponding experimental results of each specimen were compared with the present work to identify the influence of change of conical specimen materials towards level of energy absorption capacity. It is clear that the GFRP 15° conical shell have gained higher load resistance capacity than GFRP 18°&21°conical shells, and the GFRP15° conical shells also offer higher load resistance as compared

with GFRP18°&21°. The comparison of energy absorption levels of the corresponding specimens. It was observed that the energy absorption capacity of GFRP15° specimen is better when compared with the performance level of GFRP18°&21°. By Conducting Crushing Test & Analysis on E-Glass Fiber Reinforced Polymer conical Frustum with different Halfcone angles 15°, 18°&21°.

- For15° failure occurs at 26.640KN,
- For18° failure occurs at 20.492KN,
- For21° failure occurs at 11.312KN.

By the Results obtained it can be concluded that the crushing stresses induced in all frustums are within their allowable limits. And it also can be observed that the frustum which develops less vonmises stress exhibit compare to total deformation analysis on frustums.

The halfcone angle 15°

- Much stronger than26% of 18° halfconical frustum,
- Much stronger than150% of 21° halfconical frustum.

The halfcone angle 18°

- Less stronger than26% of 15° halfconical frustum,
- Much stronger than90% of 21° halfconical frustum.

The halfcone angle 21°

- Less stronger than150% of 15° halfconical frustum,
- Less stronger than90% of 18° halfconical frustum.

Considering in both deformation & stresses among all the above investigations that the 15° halfcone angle frustum is more withstand compare to 18°&21°halfcone angle frustums.

#### REFERENCES

- [1]. [1] FERREIRA JM, CHATTOPADHYAY A. AN OPTIMIZATION PROCEDURE FOR MAXIMIZING THE ENERGY ABSORPTION CAPABILITY OF COMPOSITE SHELLS. MATH COMPUT MODEL1994.
- [2]. [2] Mamalis AG, Manolakos DE, Demosthenous GA, Ioannidis MB. Analytical modelling of the static and dynamic axial



- collapse of thin-walled fibre glass composite conical shells. Int J Impact Eng 1997.
- [3]. Tong Liyong, Tsun Kuei Wang. Buckling analysis of laminated composite conical shells. Composite Science Technology.
- [4]. Shadmehri F, Hoa SV, Hojjati M. Buckling of conical composite shells. Compos Struct 2012.
- [5]. Morthorst Marion, Horst Peter. Crushing of conical composites shells by a numerical analysis of the governing factors. Aerosp Sci Technol 2006.
- [6]. Ochelski Stanislaw, Gotowicki Pawel. Experimental assessment of energy absorption capability of carbon–epoxy and glass–epoxy composites. Compos Struct 2009.
- [7]. Mamalis AG, Manolakos DE, Ioannidis MB, Papapostolou DP. Crashworthy characteristics of axially statically compressed thin-wall square CFRP composite tubes: experimental. Compos Struct 2004.
- [8]. Alkateb M, Mahdi E, Hamouda AMS, Hamdan MM. On the energy absorption capability of axially crushed composite elliptical cones. Compos Struct 2004.
- [9]. Mahdi E, Sahari BB, Hamouda AMS, Khalid YA. An experimental investigation into crushing behaviour of filament-wound laminated cone–cone intersection composite shell. Compos Struct 2001.
- [10]. Mahdi E, Hamouda AMS, Sen AC. Quasi-static crushing behavior of hybrid and non-hybrid natural fibre composite solid cones. Compos Struct 2004.
-